Cement and Concrete Research 38 (2008) 727–736

Contents lists available at ScienceDirect

Cement and Concrete Research

journal homepage: http://ees.elsevier.com/CEMCON/default.asp

Effect of a high calcite filler addition upon microstructural, mechanical, shrinkage and transport properties of a mortar

Y. Benachour [a,b], C.A. Davy [b,*], F. Skoczylas [b], H. Houari [c]

[a] Laboratoire de Génie Géologique, University of Jijel, BP 98, Ouled Aissa, Algeria
[b] Laboratoire de Mécanique de Lille, CNRS UMR 8107, and Ecole Centrale de Lille, BP 48, 59651 Villeneuve d'Ascq Cedex, France
[c] Laboratoire de Matériaux et Durabilité des Constructions, Route Ain El bey, University Mentouri of Constantine, Algeria

ARTICLE INFO

Article history:
Received 25 June 2007
Accepted 25 February 2008

Keywords:
Waste management
Filler
Mixture proportioning
Transport properties
Mechanical properties

ABSTRACT

Sands produced from limestone rock deposits in Algeria contain high proportions of fine 0/100 μm particles (named *filler* hereafter), which are available in large quantities. This study aims to identify the maximum filler amount which may be added to cementitious materials without performance loss. Performance is quantified here as related to varied properties, either microstructural (density, porosity, pore size distribution, capillary absorption, Klinkenberg effect), mechanical (Young's modulus, compressive and flexural strengths), or indicative of durability (intrinsic gas permeability, drying shrinkage and mass loss). To that purpose, mortars with various amounts of filler, ranging from 15 to 45% sand mass (i.e. 45 to 135% cement mass), have been formulated, tested and compared to a reference mortar. As recommended by J. Baron [J. Baron, Les additions normalisées pour le Béton, Les bétons - Bases et données pour leur formulation, Association technique - industrie des liants hydrauliques (in French), Eyrolles Ed., Paris, 1996, pp. 47-57], substitution to sand is privileged, whereby cement proportion and workability are kept constant while water need varies with increasing filler amount. Preliminary XRD analysis of filler powder shows no other minerals than calcite $CaCO_3$ and traces of dolomite $CaMg(CO_3)_2$. Results point out the existence of an optimal performance value and a high effect of filler addition. In particular, for high filler amounts, total porosity increases while bigger pore populations diminish. This is confirmed by SEM examinations of the microstructure as well as by the increase of Klinkenberg coefficient β determined from gas permeability measurements, and by capillary absorption results. Moreover, intrinsic gas permeability, compressive and flexural strengths remain remarkably high whatever the filler proportion. Drying shrinkage and mass loss are not impacted dramatically either.

1. Introduction

Industrial by-products such as fly ash, silica fume or blast furnace slag have helped improve concrete performance thanks to their hydraulic and/or pozzolanic activity. They are now widely used as additives to durable and high performance concretes [1–3]. Nevertheless, their cost is relatively high compared to calcareous additives (these are also named *mineral additives* hereafter). Besides, the demand for aggregates to produce concrete is still high while natural resources decrease or are being more and more regulated due to environmental concerns [8,9]. At the same time, fine 0/100 μm calcareous aggregates (named *fillers* or *calcareous fillers* hereafter) are available in great quantities as crushing residue, so that their valorisation remains a recurring economical issue, particularly in Algeria [9–11].

Additions are simply defined by the European Standard ENV 206-1 (2004) for concrete conformity as "materials made of finely divided minerals which can be added to concrete in order to improve some of its properties". Type I additives are labelled "almost inert" while Type II additives are "pozzolanic or latent-hydraulic minerals". Various countries limit quite tightly Type I addition amounts in aggregates adapted to concrete (or mortar) (Table 1). European Standards relating to aggregates for concrete (EN 12-620, 2003) or mortars (EN 13-139, 2003) allow respectively up to 22% filler in mass as an aggregate component or 5% filler in mass for a medium sand of fineness modulus FM = 2.5 (and up to 30% in mass +/−3 for very coarse sands of fineness modulus FM between 2.4 and 3.6). In parallel, French specification NF P 15-301 (1995) allows up to 5% filler only as a cement substitute, and up to 35% calcareous filler additive provided the remainder hydraulic material is pure Portland cement [4]. Despite such positive evolutions of the normative context, current formulation methods do not help anticipate filler influence and hence optimize the concrete mix. Whereas a positive filler effect is accounted for when substituting filler to sand [5], these methods are based on using fillers as cement substitutes. Industrially, when crushed aggregates are produced with a higher filler ratio than within the standard limits, these are washed before use, which remains costly and proves to weaken the aggregate-to-cement bond [6,7].

Concrete performance loss is mainly due to clay-based minerals. Their presence weakens the bond between cement paste and

* Corresponding author: Tel.: +33 3 20 33 53 62; fax: +33 3 20 33 53 52.
E-mail address: catherine.davy@ec-lille.fr (C.A. Davy).

0008-8846/$ – see front matter © 2008 Elsevier Ltd. All rights reserved.
doi:10.1016/j.cemconres.2008.02.007

Table 1
Admitted crushed filler proportion in aggregates adapted to concrete (and mortars), according to various countries

Country	Germany	Canada	Italy	Belgium	USA	France	Algeria	United Kingdom
Standard Reference	DIN 4226	CSA A231	Uni 7 163	NBN 589-102	ASTM C33	NF P 18 541, 301, X 540	DTR BE 2-1	BS 822
Date Issued	1971	1973	1972	1969	1997	1994–1983–1997	1991	1992
Sand mass %	<4%	<3–5%	<3–5%	<3–5%	<5–7%	12 to 18%	<10%	<16%

Expressed in sand mass %.

aggregates and delays cement hydration [7], [12,13]. Clay may swell, induce fracturing and hence strength loss [13]. Fortunately, on the building site as well as in the lab, the organic material content, and, hence, the clay-based material content in an aggregate may be determined simply by the Methylene Blue Test as prescribed by the European Standard EN 933-9 [14,15]. Nevertheless, drying shrinkage has to be limited when using any addition to concrete. As for them, silt and other mineral fillers such as powders of quartz, calcite, rutile and alumina [23,24], although relatively chemically inert and dissimilar to clay, have a high specific surface and hence high water-retention capacities that may cause high shrinkage without due precaution [7,12]. In a cement-based filler-added material, without any superplasticizer, the amount of free water is diminished, and most of the water is adsorbed on the surface of the filler particles or entrapped inside flocks of particles [21]. Therefore, depending on the fineness and morphology of the filler, the water need (i.e. the water-to-cement ratio) may vary as hugely as from 1 to 4 [8,16,40]. As J. Baron recalls in [5], filler addition is positive provided fillers contribute to lessen the water need, i.e. the water-to-cement ratio. The presence of mineral fillers also modifies the concrete consistency (or *workability*) [7–9,17]. The adsorbed water at the filler particle surface does not only fill up voids, it also provides greater thickness to the water layer around particles, which diminishes viscosity, and, hence, flow properties and workability in particular. For these reasons, we perform filler additions at constant practical consistency, and drying shrinkage and mass loss are assessed in parallel with mechanical performance.

According to French Standard NF P 18-508 and to EN 206-1 (2004), calcareous additions are attributed an activity index, defined as the ratio of the compressive strength σ_{UCS} of a mortar formulated with 75% cement and 25% filler (in mass) to that of a reference 100% cement mortar. Moreover, French Standard XP P18-305 for ready-mixed concrete requires a water-to-equivalent hydraulic binder (W/C_{eq}) ratio to be used, so that $C_{eq}=C+0.25F$ for the addition of a calcareous filler amount F representing up to 25% of the cement amount, and provided that its 28 day activity index is above or equal to 0.71 [41]. This is the recognition of a calcareous filler activity when added to the concrete mix. Indeed, apart from having a quite limited chemical interaction with hydration products [40], calcareous filler powder has a catalytic, and also a physical effect during cement hydration. First, it has been shown [18–20] that a chemical reaction of calcite $CaCO_3$ with C_3A and C_4AF occurs during cement hydration, contrarily to siliceous fillers, such as crushed quartz, which are reputed to have no chemical activity during cement hydration due to their high-crystallized silica content [21–23]. C_3A and C_4AF reactivity appears to increase with limestone fineness [40]. Péra et al. [25] also observed an acceleration of C_3S hydration using 10 to 50% limestone (as cement replacement) at a given Blaine fineness of 680 m^2/kg. Yet the extent of calcareous filler chemical activity is generally admitted to be very limited [40]. Ramachandran [26] has shown a nucleation role for $CaCO_3$ as well as its incorporation into the calcium silicate hydrates (C–S–H) themselves, which benefits the cement paste structuring. The catalytic effect of calcareous filler powder is due to its high specific surface, which serves as additional nucleation sites for cement hydration products [4,24,37], whereby chemical reactions are accelerated [25] and the C–S–H crystal size is diminished [9,17,43]. During this process, some calcareous particles become integrated into the cement paste [21]. Thirdly, calcareous fillers undoubtedly have several physical effects. As filler generally replaces cement there is a *dilution effect*, i.e. the cement paste amount decreases so that the compressive strength is not improved [23,25]. To avoid this effect, the cement content of our mortars is kept constant. Up to a certain amount, the insertion of fine filler particles allows denser packing of the cement paste: this is usually called the *filler effect* [5,21,44]. The filler presence also reduces the *wall effect* in the transition zone between the paste and the aggregates: this weaker zone is strengthened due to the higher bond between cement paste and aggregate, so that the concrete microstructure and properties are improved. For instance, and despite using fillers containing of up to 2.1% argillaceous particles, Topcu et al. [7] determine an optimal 7 to 10% filler addition as regards the improvement of permeability and mechanical performance of concrete. Celik et al. [8] provide similar results. These phenomena are strongly influenced by the particle size distributions (PSD) of the filler and of the aggregates [27,40]. For instance, a high size ratio between filler and aggregates induces a denser cement paste, and improved strength [21].

In order to investigate cementitious material performance with a high proportion of calcareous filler, a model mortar was formulated with various amounts of 0–100 μm calcareous powder, ranging from 15 to 45% of the initial sand mass, which represents 45 to 135% of the cement mass (Table 2), i.e. higher amounts than all current regulations authorize. A reference mortar with 0% filler is used for comparison purposes. Apart from the local material reuse issue, several elements contribute to this study originality. First, the mineral filler nature is thoroughly characterised in order to check for the absence of clay, and to compare its grain size distribution to that of cement powder. Contrarily to Topçu et al. [7] and Tsivilis et al. [28], the filler powder used here is devoid of any argillaceous mineral: X-Ray Diffraction results prove it is calcareous only. Despite investigating a variety of concrete properties, Celik et al. [8] have not checked for the presence of clay when studying the effects of crushed stone dust additions of up to 30% of the initial sand mass, and consistency was not kept constant for all formulations. Secondly, our methodology goes along the lines suggested by J. Baron [5], in the sense that workability is kept constant (for industrial practicality) by varying the water content, and calcareous powder is substituted to sand, which aims at improving the mortar performances and proposing an optimal filler/sand ratio. Nevertheless, contrarily to Baron, we chose to keep cement content constant and solely investigate the effect of hugely increasing the filler proportion. Indeed, studies concerning substitution to sand are scarce [7,8,17], contrarily to those devoted to cement substitution [21–23,28,29,42]. Cement content is identical for all mortars (at 450 kg/m^3), whereas water amount is varied in order to account for water need variations when adding filler powder. As a consequence, water-to-cement ratio (W/C) varies in the range 0.46 to 0.67. Fineness modulus is also evaluated and compared with water need. Topçu et al. [7] have imposed a constant workability, measured by slump test, while our study considers spreading time measurements (NF P 18-

Table 2
Physico-chemical composition of the filler powder used in this study

	CaCO3 (%)	Blaine fineness value (m^2/kg)	Methylene blue value MBF (g/100 g)	Water content Wf (%)	Fe (%)	MgCl (%)	Cl (%)
Mean	98.50	375.97	0.58	0.00	0.00	0.35	0.01
Standard deviation	0.36	30.45	0.10	0.00	0.00	0.17	–

452, NF P 15-437 or [30]). They have given performance results for less than 15% mineral powder addition only, whereas our study involves amounts of up to 45% of the initial sand mass. Moreover, Topçu et al. [7] have varied the cement content in the low range (200 to 350 kg/m^3) and the water to cement ratio (W/C) in the higher range of 0.6 to 0.98. Apart from compressive and flexural strength identification, they provide simplified durability evaluation, as their permeability tests were not fully conclusive. In our study, and complementarily to mercury intrusion porosimetry (MIP) and SEM analysis, capillary absorption measurements have allowed investigation of the influence of filler upon the porous network structure and size. Celik et al. [8] evaluate absorption after 72 h water immersion only, using a simplified technique, and these are not correlated with density or porosity measurements. Ushikawa et al. [17] have substituted various mineral powders to fine aggregate and kept cement proportion constant, yet they have also kept water amount constant and the mineral powder proportion is adjusted so that the unit volume of all powders including cement is kept constant. Similarly, Bédérina et al. [9] optimize their concrete mix at given volume and cement proportion (350 kg/m^3), so as to obtain a maximum dry mix density. Despite getting optimal compactness, superplasticizer is required and water-to-cement ratio (W/C) has to be of up to 0.6 in order to maintain proper workability. Tsivilis et al. [28] have focused upon durability properties of Portland limestone cements, i.e. cement substitution. They have identified intrinsic gas permeability coupled to water absorption and pore structure analysis using MIP and optical microscopy. Yet clay amounts are accounted for, plasticizer has been used for 2 of the 14 formulations tested in order to keep a proper workability, the water-to-cement ratio is quite high (0.65) and the cement proportion rather low (300 kg/m^3).

Hereafter, varied experimental tools have been used in parallel. This aims at better understanding microstructural modifications due to the presence of filler powder, namely porosity and particle size distribution (PSD), and their consequences upon physical, mechanical and transport properties, i.e. capillary absorption, drying shrinkage and mass loss, Young's modulus, compressive and flexural strengths, and gas permeability. The Klinkenberg effect is also evaluated from gas permeability measurements. Where capillary absorption and Klinkenberg effect give insights into global pore structure and volume [31], mechanical testing provides mechanical performance estimation, while shrinkage and permeability are used as durability indicators.

2. Experimental procedure

2.1. Materials

Mortars are formulated using normalized sand, as described by EN 196-1, CEM I 52.5 cement, as described by EN 197-1, and 0 to 100 μm calcareous filler powder produced by the Boulonnais Quarries (Rinxent, France). Table 2 displays several filler characteristics, as provided by the manufacturer: calcite $CaCO_3$ is in majority (with 98.5%), dispersed with a few magnesium and chlorine atoms (less than 0.5%). Its Blaine fineness value (375 m^2/kg) is on the order of that of cement (usually of 300 to 500 m^2/kg [4]) so that their water need is similar. X-ray diffraction results for filler powder confirm the presence of calcite $CaCO_3$, added with calcareous dolomite $CaMg(CO_3)_2$, (Fig. 1). In particular, this attests that no undesirable argillaceous component is present in the filler powder. This is in accordance with the Methylene Blue Value of 0.58 g/100 g for the calcareous filler used (Table 2), the specified limit indicative of water sensitivity for an aggregate being above 1 g/100 g (NF P 18 508). Particle size distributions (PSD) for cement and filler powder are determined by laser granulometry (Fig. 2). Both cement and calcareous powder have similar PSD curves, with coefficient of curvature $Cg=(d_{30}^2/d_{60}*d_{10})$ equal to 1.1 for the filler powder and 1.5 for the cement powder (well-graded powders are in the range 1–3). Yet, cement PSD is narrower, with a uniformity (or Hazen) coefficient $CU=(d_{60}/d_{10})$ of 6.2 compared to 12.4 for the filler powder. Indeed, filler powder has a larger population of smaller grains than cement in the range 0.4 to 30 μm. This is interpreted in favour of an ability of filler powder to fill in voids or interfaces between cement and sand [21].

2.2. Experimental methodology

2.2.1. Mortar and sample preparation

Mortars with various filler proportion have been made up by a trial-and-error process, so as to get a constant workability of 25 sec+/−1, measured using a B-type workability meter, as defined in French Standard NF P 18-452 and NF P 15-437 [30]. This process includes air bubble removal using a vibrating table. Reference mortar, without filler added, is chosen with a water-to-cement ratio of 0.48. Preliminary workability measurements are performed with Vicat's apparatus

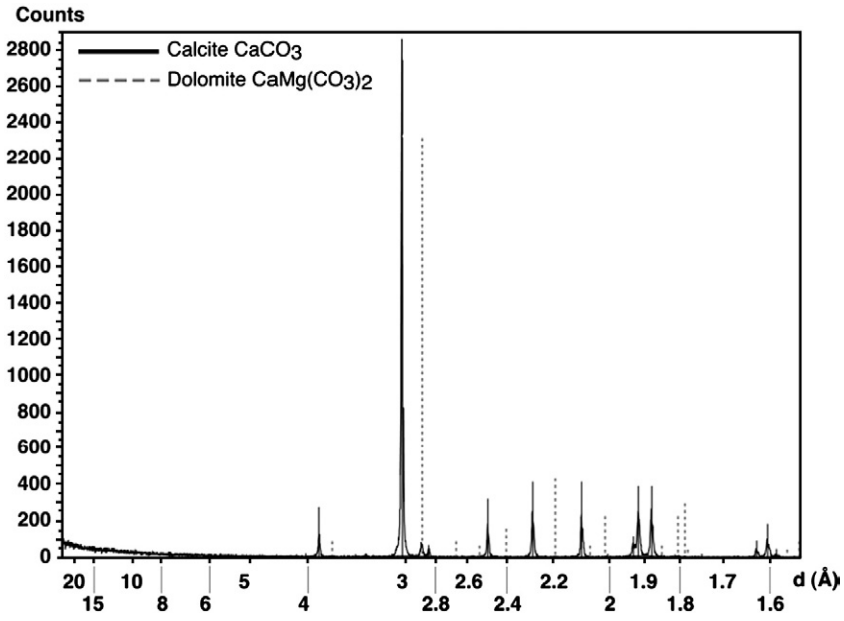

Fig. 1. X-Ray Diffraction results for filler powder showing the presence of calcite $CaCO_3$ and dolomite $CaMg(CO_3)_2$.

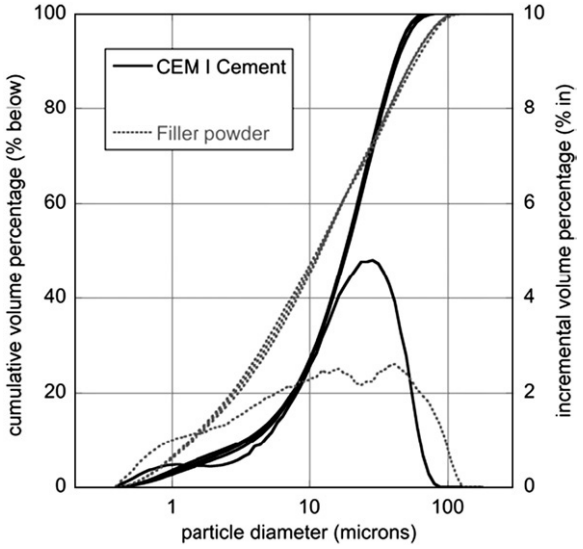

Fig. 2. Particle size distribution (PSD) for CEM 1 cement and filler powder obtained by laser granulometry.

[4], because it allows formulating much smaller mix amounts than with B-type workability meter. With Vicat's apparatus, $W/C=0.5$ mortar does not have a measurable workability, hence, a smaller $W/C=0.48$ is preferred for reference mortar. After Vicat's workability tests, all formulations are checked for constant consistency at a larger scale with B-type workability meter (i.e. larger amounts of mortars are tested). Investigated filler proportion are 15, 25, 35 and 45% of the reference mortar sand mass, which corresponds to 45–135% of the cement amount.

After mixing them all on the same day, mortars are cast into $50\times15\times15$ cm^3 or $4\times4\times16$ cm^3 prismatic forms, and protected from desiccation using plastic sheets. After 24 h hardening, all mortar prisms are removed from their forms and immersed in water at 20 °C+/−1 for 28 days. $50\times15\times15$ cm^3 mortar prisms are cored, cut to length and rectified for end surface parallelism. Density ρ and porosity ϕ are average values measured on five 37 mm diameter discs, with a height of 10, 20, 30, 40 and 60+/−5 mm for each mortar (i.e. 5 samples per mortar). Height variation aims at checking for potential structural effects upon ρ and ϕ. MIP specimens are taken from 2 months or one year old mortars preserved in lime-saturated water. Flexural failure tests are performed on $4\times4\times16$ cm^3 prismatic samples after 28 days hardening. Right after failure, flexural test samples are used to perform compressive strength measurements. Young's modulus and permeability measurements are performed on circular cylindrical samples of 37 mm diameter and a length/diameter ratio (L/D) of 2 in order to limit end effects. Capillary absorption testing requires $4\times4\times16$ cm^3 prismatic samples, taken after 7 days hardening. Shrinkage and mass loss samples are $2\times2\times16$ cm^3 prisms. They are tested after 6 months storage in lime-saturated water. All sample sizes are significant compared with the sand aggregate maximum size of 2 mm.

2.2.2. Fineness modulus, density and porosity measurement techniques

When each formulation was determined as explained above, the (sand+filler) dry mix was reconstituted and passed through a sieving machine, in order to determine the mix fineness modulus FM according to the procedure provided by French Standard NF P 18 540. FM is defined as the sum of the cumulative refuse percentage, divided by 100, for the sieves of modulus 23, 26, 29, 32, 35, 38, i.e. 0.160, 0.315, 0.63, 1.25, 2.5 and 5 mm nominal dimension. An additional 0.08 mm sieve was used in order to separate a minimal amount of filler particles.

For each mortar, density and porosity are evaluated at 28 days hardening. Density is measured after mass stabilisation of each sample placed at 65 °C, from weighing and specimen dimensions measurement (for the volume). Samples are then water-saturated under vacuum in order to deduce porosity from the mass of water their pores contain. Additionally, mercury intrusion porosimetry measurements are conducted upon 1 cm^3-sized samples of each mortar using a MICROMERITICS© AutoPore IV 9500 device.

2.2.3. Mechanical testing techniques

After 28 days hardening, flexural failure tests and compressive strength tests are performed as recommended by ASTM 116-90 and EN 196-1. Young's modulus is also measured after 28 days hardening. We use a four LVDT sensors device, for use on a typical mechanical testing machine, as designed by our laboratory [32]. Parasitic bending effects are limited thanks to a swivel joint placed between the machine mobile platen and the sample, and axial displacement is averaged using four LVDT sensors. These are placed between two rings fixed at a 30 mm initial distance on the sample. Preliminary results show a good agreement with longitudinal strain gauge measurements.

2.2.4. Permanent gas permeability technique

Gas permeability measurements are performed on initially dried samples, taken after mass stabilisation at 65 °C. Results are averaged on three tests performed on two different samples. Each sample is wrapped in a Viton membrane and placed inside a triaxial cell, where it is confined at a constant hydrostatic pressure of 5 MPa *via* HF95Y Enerpac™ hydraulic oil (Fig. 3). Simultaneously, inert Argon gas is

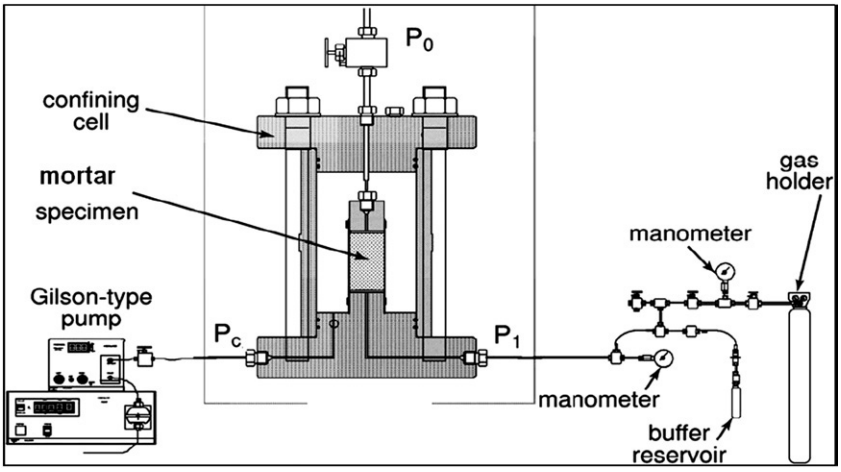

Fig. 3. Sketch of the triaxial cell displaying the associated permeability measurement set up.

Table 3
Relationship between salt-saturated solution and relative humidity (source: OIML)

Saline solution	K_2SO_4	KCL	IK	NaBr	K_2SO3	$KCH_3\ CO_2$
RH (%) at 20 °C	97.6±0.5	85.1±0.5	69.9±0.5	59.1±0.5	43.2±0.5	23±0.5

injected through a buffer reservoir to the bottom sample side at a given pore pressure P_i of 1.1, 2.1 or 3.1 MPa (absolute pressure values). Gas flows down to the sample upper side, which is open to atmospheric pressure P_0. When gas flow is permanent, its inflow is stopped down before the buffer reservoir, in order to get a small pressure decrease ΔP of up 0.01 MPa on the sample bottom side. The time Δt to obtain ΔP is recorded. Apparent gas permeability K_{app} is then deduced from Darcy's law, from the assumption that Argon gas is a perfect gas, and that the gas flow from the buffer reservoir down to the sample upper side remains quasi-permanent at an average pressure $P_{mean}=P_i-(\Delta P/2)$. The corresponding equation writes:

$$K_{app} = (2\mu LV_1 \Delta P)/(A\Delta t(P_{mean}^2 P_0^2)) \quad (1)$$

where μ is Argon gas viscosity, taken as 2.2×10^{-5} Pa sec, L is the sample length, V_1 is the buffer reservoir volume, and A is the sample cross sectional area [33,34].

The existence of an apparent permeability is due to gas particles slippage on the pore surface, which modifies permeability values with varying gas pressure [35]. Indeed, Darcy's law assumes a non-sliding contact of fluid at the pore surface (laminar fluid flow). Sliding is taken into account using Klinkenberg equation:

$$K_{app} = K_{int}(1 + \beta/P_m) \quad (2)$$

where K_{int} is the porous material intrinsic permeability, β is the Klinkenberg coefficient and $P_m=(P_i+P_{atm})/2$ is the average pressure inside the sample. It is shown that β depends linearly on the inverse of the average material entry pore radius, i.e. the higher β, the smaller the average pore size [35]. By varying pore pressure P_i, intrinsic permeability K_{int} and Klinkenberg coefficient β are deduced from (Eq. (2)).

2.2.5. Capillary absorption technique

The evaluation of capillary absorption for a porous material provides global insights into its porous structure and volume [31]. Following French Standard NF P 18 354 (1986), each test consists in measuring the average water amount (i.e. mass) absorbed by three identical samples after a given time. After 24 h hardening, samples are stripped and kept in a 50% relative humidity (RH) atmosphere (±5%) at 20 °C. A relative humidity of 50% is prescribed by NF P 18 354 because, at such a low value, the transition from capillary phenomena to water adsorption (upon the pore surface) is reached. Indeed, combining Kelvin's law ($p_c=-\rho_l$ RT ln(RH)/M_v with $\rho_l=100$ kg/m^3 and $M_v=0.018$ kg/mol for liquid water, $R=8.34$ J/K/mol, T in Kelvins) and Laplace's law for capillarity ($p_c=2\gamma/r$ with surface tension $\gamma=7.275\ 10^{-2}$ N/m for liquid water/air) at RH=50%, provides a pore diameter of 3.09 nm where the capillary meniscus is present, which corresponds to about 11 to 12 water molecules (a water molecule has a diameter of 2.6 to 2.8 Angströms). Below a tenth water molecules, capillarity does not describe the behaviour of poral water: we reach the domain of adsorption and disjunction pressure [39].

At 7 days of age, samples are weighed, and then placed vertically in a container filled with a 2 cm-thick layer of 0 to 0.5 mm water-saturated siliceous sand. For each further weighing, prisms are taken out of the container, wiped on their surface, weighed, and then replaced on the sand bed. Weighing occurs every 2 h for 8 h, then every day for the next 7 days. From these measurements, capillary absorption coefficient Ca is defined at time t as the ratio of sample mass variation to the sample cross-sectional area A:

$$Ca(t) = (m(t) - m(t=0))/A \quad (3)$$

where $m(t)$ is the sample mass at time t. Ca(t) is usually plotted as a function of the square root of time [38].

2.2.6. Drying shrinkage and mass loss measurements

Two specimens of each mortar are equipped with studs at both ends, as recommended by NF P15-433 and NF P18-427. They are placed inside an hermetic chamber, above a salt-saturated solution at given relative humidity RH at 20 °C. A calibrated retractometer provides length values as measured between the studs and samples are regularly weighed. By changing the salt solution after mass and length value stabilisation, relative humidity is varied from 97.6% down to 23% (Table 3).

3. Results and discussion

3.1. Mortar formulations

The mass proportioning for all filler-added mortars is given in Table 4. Proportions given for reference mortar correspond to 1 m^3 material. While filler amount increases up to 15% sand mass, water need, i.e. (W/C), decreases, and it becomes greater by up to 40% for higher filler amounts. Water is getting adsorbed at the surface of filler particles. As filler specific surface is higher than that of sand, water demand increases due to the adsorption phenomenon. At the same time, filler particles fill up voids so that water has less pore space available. On the whole, less free water is present whereas the amount of adsorbed water increases. These opposite effects lead to a decrease in water need up to around 15% filler and a regular increase above this value. (W/C) increase will induce higher porosity. Therefore, lower strength, higher drying shrinkage and gas permeability (measured on dried material) are expected above 15% filler addition. If calcareous filler is granted an activity in the cement mix, as in French Standard XP P18-305, it has to be accounted for in $(W/C_{eq})=W/(C+0.25F)$, see Section 1, at least for filler amounts F representing up to 25% cement mass, and even if filler is substituted to sand. Fig. 4 represents (W/C+0.25F) along (W/C) with increasing filler amount: the actual water need (W/C_{eq}) to take into account for any filler proportion is situated between those boundaries. The above conclusions remain: the water need decreases up to about 15% filler, and monotonously increases above this value, yet it is in lower proportion than when considering

Table 4
Composition of mortars added with filler (mass proportioning)

Filler addition		Normalized sand	CEM I 52.5 cement	Water (litres)	W/C ratio	Filler-to-cement proportion (cement mass %)	Sand+filler fineness modulus FM	B-Type workability meter NF P 18-452 (s)
(%)	(kg)	EN 196-1 (kg)	EN 197-1 (kg)					
0	0	1350	450	216	0.48	0	2.37	
15	202.5	1147.5	450	210	0.467	45	2.33	
25	337.5	1012.5	450	231	0.513	75	1.85	25±1
35	472.5	877.5	450	275	0.611	105	1.59	
45	607.5	742.5	450	302	0.671	135	1.38	

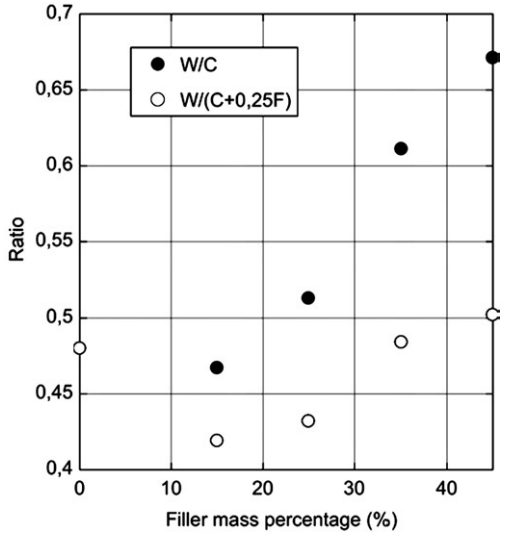

Fig. 4. Variation of W/C and $W/(C+0.25F)$ ratios as a function of filler rate.

(W/C) only. The actual water need (W/C_{eq}) may increase between only 4% and up to 40% of its initial value with increasing filler amount. The effect of filler addition upon material performance and durability might not be as obvious as expected.

Fineness modulus FM decreases hugely with filler amount from 2.37 (for the reference mortar) down to 1.38 (45% filler-added mortar), which represents more than 40% decrease (Table 4). Despite this, the aggregate mix remains conform to European Standards (EN 12620, August 2003, for concretes and EN 13139, August 2003, for mortars) up to more than 35% filler proportion: boundaries are of 1.5 to 2.8 for a medium normalized sand of fineness modulus 2.5. The increase in fineness is proven to enhance water need and cement hydration [23,24,40](Section 1), hence, we expect it to have an effect upon mortar performance and durability.

3.2. Effect of filler addition upon mortar microstructure

3.2.1. Density, porosity and pore size distribution as given by MIP

Average, minimum and maximum values for density ρ are given in Fig. 5 for each filler proportion. These show that the structural effect due to varying specimen dimensions is limited. The filler effect is obvious, whereby mortar densifies up to an optimum value situated between 0 and 25% filler amount. For higher filler amounts, density looses only by 6.8% of its reference value (at 45% filler). Similarly, and although at given dry mix total volume and cement amount, Bédérina et al. [9] show a density increase of the dry mix up to an optimal value of filler amount which represents 9 to 16% sand mass (depending on the sand PSD), and a regular decrease for higher proportions. This is interpreted as filler powder first filling voids around sand grains, up to the optimum. For higher filler amounts, those voids being completely filled, filler powder occupies the place of sand grains, hence diminishing sand proportion, and consequently the mix density.

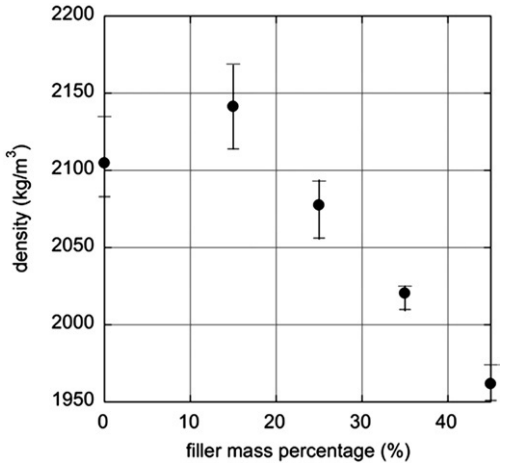

Fig. 5. Variation of density as a function of filler mass percentage.

Porosity ϕ values are represented Fig. 6, as obtained by two methods: MIP on two-months-old or one-year-old samples, or water saturation under vacuum. Porosity remains stable (except for one year old samples) for filler percentages of up to 15% sand mass, whereas it almost doubles when reaching 45% filler. Porosity, being mainly due to water presence inside the mortar, follows a similar evolution to water need (W/C) (Section 3.1). Normalised pore size distributions of mortars are more interesting (Fig. 7). They are similar whether evaluated at two-months old or one-year old. The 0.1/1 μm pore population represents 17% of the total pore volume for reference mortar, whereas it only represents 2 to 5% for filler-added mortars up to 45% sand. While total porosity increases, filler addition clearly limits pore populations to lower sizes, in majority below 0.1 μm: 73% pore volume is below 0.1 μm for the reference mortar, whereas it represents 89% to 93% pore volume for filler-added mortars. This effect is referenced in [40] for a finer calcareous powder than used here (more than 50% particles below 0.1 μm). The finer pore structure is attributed to the nucleation effect: the introduction of a large number of nucleation sites could induce a more homogeneous distribution of C–S–H and, hence, a less open pore structure. This effect would be rather in the capillary pores than in the gel pores. As recalled by Bédérina [9], Ushikawa et al. [17] have shown that adding mineral powder in concrete reduces the size of hydration products, inhibits the deposit of Portlandite $Ca(OH)_2$ thanks to their filling role, and, consequently, decreases pore size.

3.2.2. SEM observations and capillary absorption

Fig. 8 displays capillary absorption results as a function of the square root of time and for different filler amounts (three samples per mortar type). Two phases may be noticed, as detailed in [38]. The initial linear phase corresponds to the filling of the bigger capillary pores, and lasts up to 4 h only. The second non-linear phase corresponds to the filling of the smaller and finer pores and lasts up to 7 days immersion. On the whole, comparable evolutions of capillary absorption are observed for filler proportions of up to 25% sand mass.

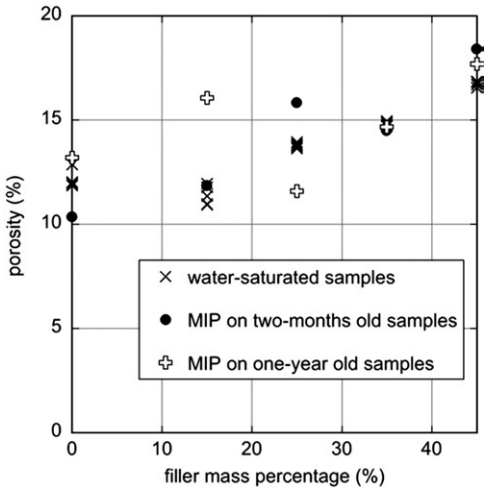

Fig. 6. Variation of porosity as a function of filler percentage. Porosity is evaluated by two different methods: mercury intrusion porosimetry (MIP) and water saturation under vacuum.

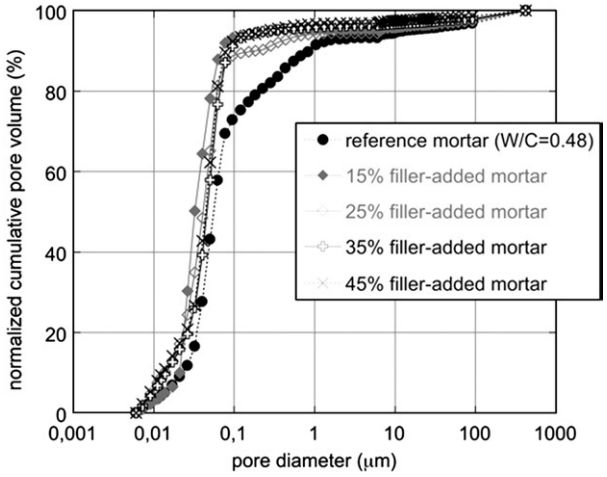

Fig. 7. Mercury Intrusion porosimetry: normalized cumulative pore volume is given as a function of pore diameter for the reference mortar and for each of the filler-added one-year old mortars.

These are moderate with capillary absorption coefficient Ca ranging from 0.52 to 0.65 g/cm^2 after 7 days immersion. With 35 and 45% filler addition, Ca notably increases with average values of 0.84 g/cm^2 and 1.27 g/cm^2 respectively after 7 days. Capillary absorption values at 45% filler are double of those at 25% filler, in accordance with total porosity increase. When considering the two successive absorption phases, it is also noticed that after the filling of the larger pores (from 4 h, i.e. $\sqrt{t}$=2 h$^{1/2}$), capillary absorption is greater for 35% and for 45% filler mass percentage rather than for 0, 15 or 25% filler addition. This means that filling of smaller pores is greater from 4 h to 7 days immersion for highly filler-added mortars, i.e. that smaller pores are more numerous with higher filler amounts. This is in accordance with MIP results.

SEM observations of unpolished mortar surfaces at 15 and 45% filler amounts are a complementary investigation means (Fig. 9a and b). Visual inspection shows that the average pore size decreases significantly between 15% filler amount and a much higher 45% filler amount. Complementarily to capillary absorption and MIP results, this contributes to show that, despite total porosity increase, high filler amounts induce a notably finer pore size population.

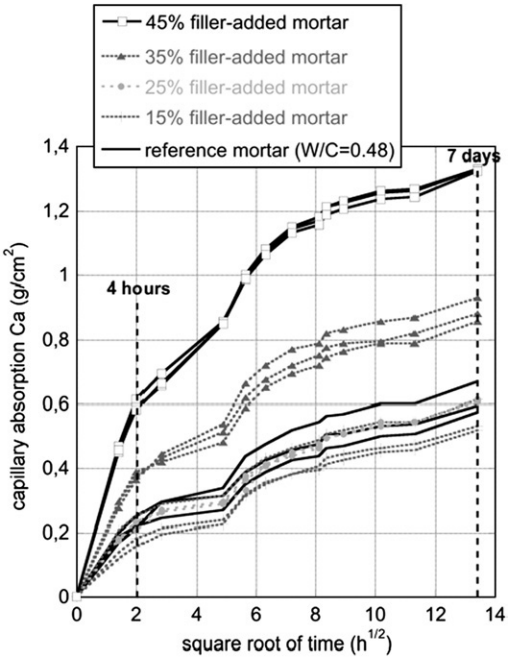

Fig. 8. Capillary absorption as a function of square root of time and filler mass percentage.

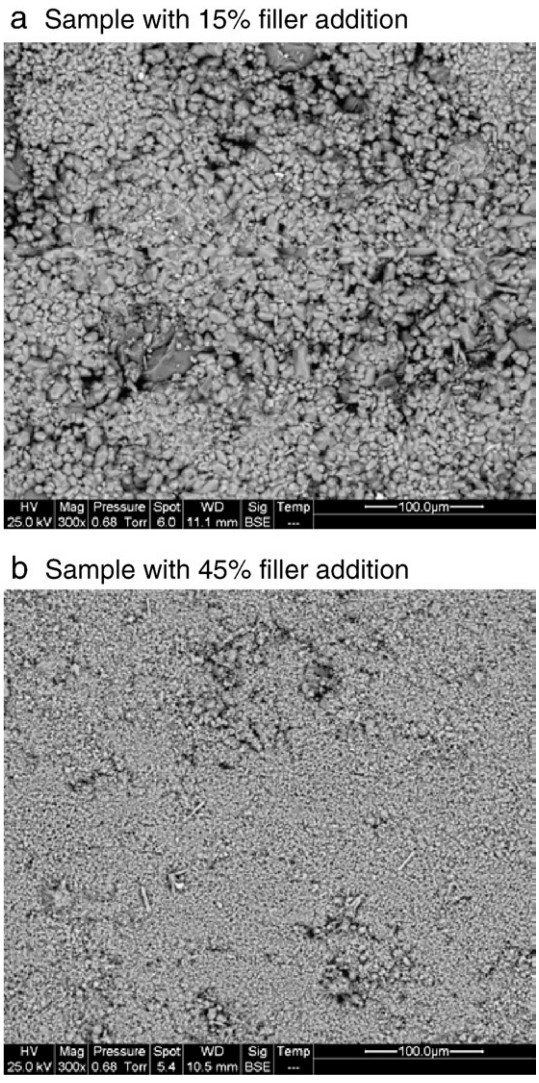

Fig. 9. SEM micrographs of unpolished mortar samples with 15% or 45% filler addition. Pores are in black and appear smaller for the 45% filler addition sample.

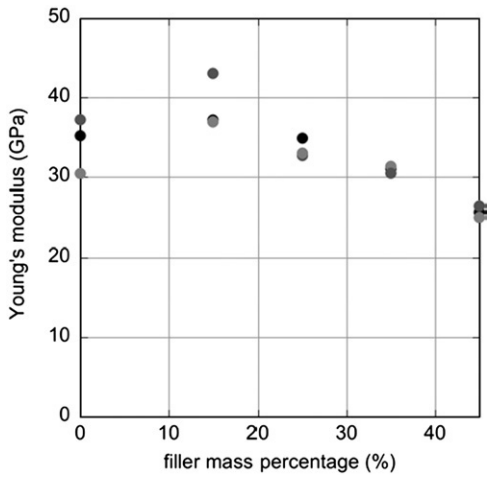

Fig. 10. Variation of Young's modulus as a function of filler mass percentage.

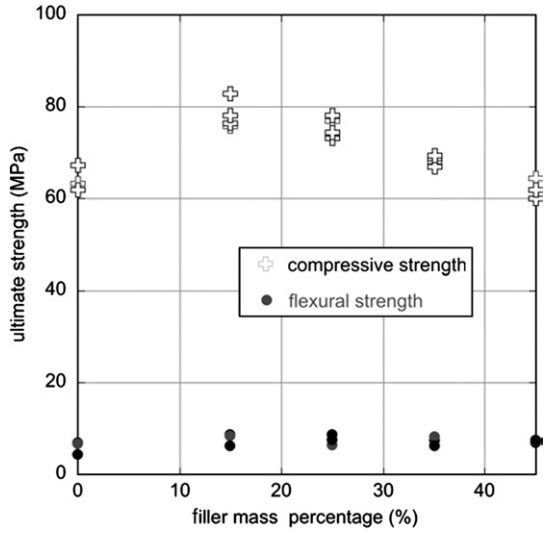

Fig. 11. Variation of ultimate compressive stress σ_{ucs} and ultimate flexural stress σ_{UFS} as a function of filler mass percentage.

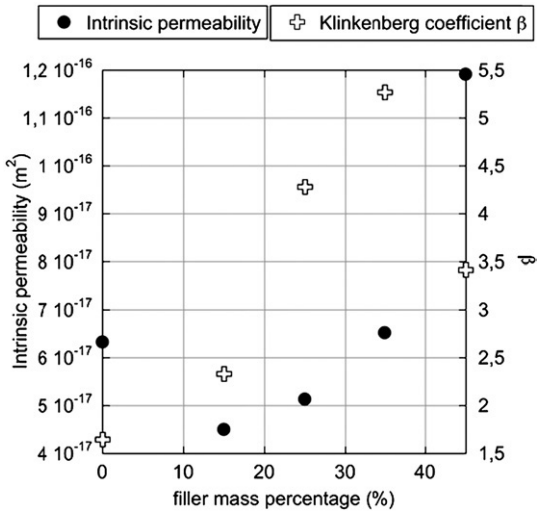

Fig. 13. Variation of intrinsic permeability and Klinkenberg coefficient β as a function of filler mass percentage.

3.3. Effect of filler addition upon mechanical performance

Fig. 10 displays Young's modulus E evolution with increasing filler proportion. This evolution follows symmetrically that of (W/C) and porosity: the higher the porosity, the more flexible the mortar is, i.e. the lower Young's modulus E is. Filler additions of up to 15% sand induce greater Young's modulus by 15%. Above 15% filler amount, E diminishes down to 23% of its initial reference value. The finer pore size distribution does not appear to influence Young's modulus.

Ultimate compressive and flexural strengths are not influenced by filler proportion in quite the same way as Young's modulus (Fig. 11). Due to its low average value (7.1 MPa), the evolution of flexural strength σ_{UFS} is less marked than that of compressive strength σ_{UCS}. Nevertheless, both ultimate compressive and flexural strengths (σ_{UCS} and σ_{UFS}) increase for filler additions of up to 15% sand mass, with increasing density and decreasing porosity. Most interestingly, σ_{UCS} and σ_{UFS} do not decrease notably above 15% filler amount. At 45% filler, σ_{UCS} is lower than the reference value by only 3%, and σ_{UFS} remains higher than the reference value by 17%. Optimal strength values are obtained between 0 and 25% filler addition, with 27% greater compressive strength and 30% greater flexural strength at 15% filler. Whereas porosity sharply increases with high filler amounts, strength evolutions are not linked with porosity solely. Several combined effects may be called upon to explain strength maintenance. In presence of filler, the solid skeleton may be strengthened thanks to a more homogeneous distribution of smaller C–S–H crystals, finer pore structure, accelerated cement hydration. The 6.8:1 size ratio between sand and filler is of influence there (d_{50}(sand)=80 μm and d_{50}(filler)=11.8 μm) [21]. Moreover, the bond between cement paste and sand particles may be strengthened thanks to the reduction of the wall effect provided by the fine particles filling [23]. On the contrary, strength loss, such as that observed here between 15 and 45% filler, is quite well explained: strength decreases with increasing (W/C) ratio, which is the case here. Celik et al. [8] observe that, beyond an optimal value of crushed stone dust addition (determined at 10% sand mass replacement in their study), the amount of fines increases so much that the cement paste is not able to coat all fine and coarse particles (i.e. filler as well as sand). This phenomenon weakens the cement-to-aggregate bond and hence leads to a loss in compressive strength for higher filler amounts than the optimal value. Yet, this is not the case

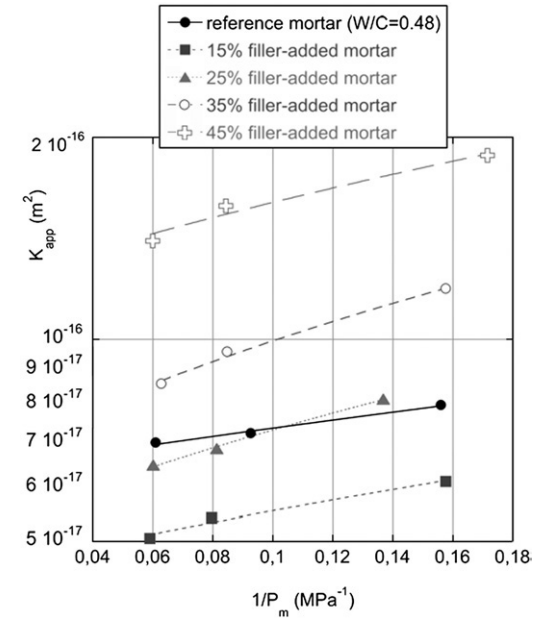

Fig. 12. Variation of apparent permeability K_{app} as a function of (1/Pm) and filler mass percentage. Lines represent the best linear fit to the data in the least squares sense.

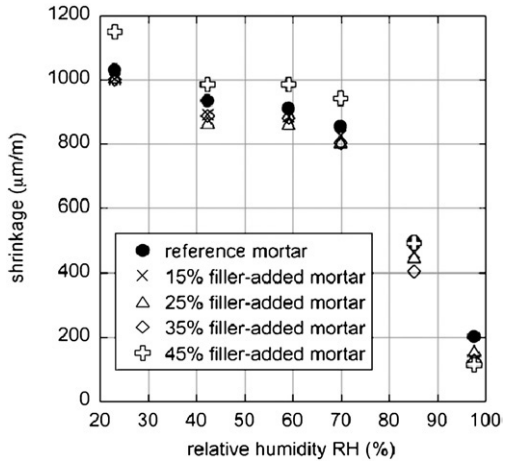

Fig. 14. Shrinkage results as a function of relative humidity and filler mass percentage.

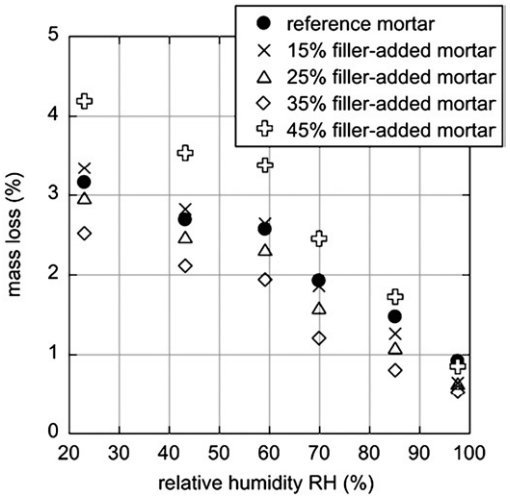

Fig. 15. Mass loss results as a function of relative humidity and filler mass percentage.

here where cement and filler have similar particle size ranges. As Kolias et al. [36] state, strength changes in cementitious materials may be attributed to the interaction of paste thickness, i.e. paste volume, bond strength and modulus of elasticity of paste and aggregates.

3.4. Effect of filler addition upon durability

3.4.1. Gas transport properties and Klinkenberg effect

Our gas permeability results on filler-added mortars are provided Figs. 12 and 13. As expected, apparent permeability K_{app} increases progressively with increasing filler amount of up to three times more than its initial value (Fig. 12). Linear interpolation from ($1/P_m$, K_{app}) plots provides intrinsic permeability K_{int} and Klinkenberg coefficient β variations (Fig. 13). Intrinsic permeability K_{int} decreases down to a minimal value of 4.5×10^{-17} m^2 at 15% filler, and then, K_{int} increases of up to 1.19×10^{-16} m^2 with increasing filler amount: this follows similar evolution to (W/C) ratio, i.e. to porosity. Indeed, Kolias et al. [36] state that the main factor influencing transport properties of concrete is its paste porosity. Celik et al. [8] observe a decrease in air content, concomitant with a decrease in water permeability, with up to 30% filler amount. They explain that filler powder blocks the passages connecting capillary pores and water channels. This blockage is affected by the amount of filler, in the sense that the more fluid passages are blocked, the more impermeable the cementitious specimen becomes. Most interestingly, K_{int} remains below or equal to the reference value (at 0% filler) for filler amounts of up to 35%. Complementarily, Klinkenberg coefficient β increases continuously up to 35% filler amount, from 1.6 to 5.2 MPa. A smaller value of 3.4 MPa is obtained at 45% filler. Yet, due to measurement accuracy, a general increase in β may be concluded from these results, which is indicative of an average entry pore size decrease. Klinkenberg coefficient evaluation is certainly not sufficient to identify an average pore size value, all the more so as its evolution with increasing filler amount is quite irregular (Fig. 13). Yet, it follows a trend (that of finer pore population), which is correlated by other results obtained with very different experimental techniques.

3.4.2. Drying shrinkage and mass loss

Drying shrinkage and mass loss results are given after 250 days test (Figs. 14 and 15). When relative humidity (RH) decreases from 97.6%, drying shrinkage is equivalent whether the mortar is added with up to 35% filler or not. For 45% filler, drying shrinkage at RH=23% is greater of 11.6% than the reference value. On the opposite, mass loss decreases with filler amounts of up to 35%, whereas it is greater than the reference at 45% filler. In terms of drying shrinkage and mass retention capacity, filler addition is not harmful for filler amounts of up to 35%.

4. Conclusion

This study aimed at helping valorise local limestone sands, which may contain high calcareous filler proportions, of up to 45% sand mass, i.e. 135% cement mass. To that purpose, filler-added mortars have been formulated by substitution to sand, with constant workability and cement amount. Microstructural, mechanical and durability properties have been investigated simultaneously using varied experimental techniques. The absence of potentially harmful clayey constituents has been checked through XRD analysis, while the fineness modulus decrease of the dry (sand+filler) mix is proven to remain within authorized standards up to 35% filler. During mortars formulation, water need ranges between the usual water-to-cement ratio (W/C) and a water-to-equivalent hydraulic binder ratio ($W/C+0.25F$) due to calcareous filler activity (French Standard XP P18-305), so that it decreases up to 15% filler, and then increases for higher filler amounts. This is the consequence of two opposite effects. On one part, water is getting adsorbed at the surface of filler particles. As filler specific surface is higher than that of sand, water demand increases due to the adsorption phenomenon. On another part, filler particles fill up voids so that water has less pore space available. On the whole, less free water is present whereas the amount of adsorbed water increases. Porosity follows similar evolution to water need. Density reaches a maximum situated between 0 and 25% filler, so that the usual *filler effect* is evidenced, and looses less than 10% of the reference value (0% filler) at 45% filler. As for them, Young's modulus and intrinsic permeability follow symmetrically the evolution of water need, i.e. of porosity. Indeed, mortar rigidity is directly driven by its porosity: when porosity increases, Young's modulus decreases, i.e. the mortar becomes more flexible. Porosity increase also provides more room for gas to pass through the mortar, which induces a corresponding increase in its permeability. Most interestingly, intrinsic permeability remains below or equivalent to that without filler, for filler amounts up to 35%. Mechanical (compressive and flexural) performance is improved by filler addition, or remains equivalent to the reference value. Optimal compressive and flexural strengths are obtained between 0 and 25% filler mass percentage. This is interpreted as being due to the void filling effect and to the cement paste strengthening (and/or to the cement paste/sand aggregate bond strengthening) allowed by the presence of filler. Along with capillary absorption and SEM results, MIP shows that a finer pore structure is obtained with increasing filler content. Following a similar trend, Klinkenberg coefficient β increase shows that, despite total porosity increases, the entry pore size diminishes. In light of this study, it is concluded that proportions of calcareous 0–100 μm fillers of up to 35% sand mass, i.e. 105% cement mass, do not affect notably the mechanical, shrinkage and transport performance of mortars, which is economically important, particularly in Algeria, but also for major European countries. Further investigations will focus upon potential chemical attacks (sea-water, acid-water, sulphate, leaching, etc.) for better durability assessment [41].

References

[1] F. De Larrard, Formulation des bétons et propriétés des bétons à très hautes performances, LCPC internal research report n.149 (in French), 1988.
[2] V. Yogendran, B.W. Langan, M.N. Haque, M.A. Ward, Silica-fume in high-strength concrete, ACI Mater. J. (1987) 124–129.
[3] M. Pala, M. Özbay, A. Özta, I.M. Yuce, Appraisal of long-term effects of fly ash and silica fume on compressive strength of concrete by neural networks, Constr. Build. Mater. 21 (2) (2007) 384–394.
[4] A.M. Neville, Propriétés des bétons, translated from English by CRIB (Sherbrooke-Laval, Canada), Eyrolles Ed., Paris, 2000.
[5] J. Baron, Les additions normalisées pour le Béton, Les bétons - Bases et données pour leur formulation, Association technique - industrie des liants hydrauliques (in French), Eyrolles Ed., Paris, 1996, pp. 47–57.
[6] F.M. Lea, Chemistry of Cement and Concrete, 3rd Ed.Edward Arnold, London, UK, 1970.
[7] I.B. Topçu, A. Ugulru, Effect of the use of mineral fillers in the properties of concrete, Cem. Concr. Res. 33 (2003) 1071–1075.

[8] T. Celik, K. Mamer, Effects of crushed stone dust on some properties for concrete, Cem. Concr. Res. 26 (1996) 1121–1130.
[9] M. Bédérina, M.M. Khenfer, R.M. Dheilly, M. Quéneudec, Reuse of local sand: effect of limestone filler proportion on the rheological and mechanical properties of different sand concretes, Cem. Concr. Res. 35 (2005) 1172–1179.
[10] Y. Benachour, Analyse de l'influence du sable de mer et du sable de carrière sur les caractéristiques du béton, Magister thesis (in French), University Mentouri of Constantine, Algeria, 1992.
[11] N. Koutchoukali, S. Adjali, Y. Benachour, Reconnaissance des sables de concassage de la région de Constantine, Proceedings of the National Seminar organised by ERCEst and CTC Est (in French), Béjaia, Algeria, 1992, pp. 99–110.
[12] P.K. Mehta, P.J.M. Monteiro, Concrete: Structure, Properties and Materials, 2nd Ed. Prentice-Hall, Englewood Cliffs, NJ, 1993.
[13] B. Felekoğlu, A comparative study on the performance of sands rich and poor in fines in self-compacting concrete, Constr. and Build. Mater. 22 (4) (2008) 646–654.
[14] N.L. Trang, L'essai au bleu de méthylène, un progrès dans la mesure et le contrôle de la propreté des granulats, Bull de liaison du LCPC n.107 (in French), 1980.
[15] A. Le Roux, Z. Unikowski, Mise en évidence des fines argileuses dans les granulats à béton, Bull de liaison du LCPC n.110 (in French), 1980.
[16] A.R. Kara, Influence des additions minérales sur le besoin en eau et les résistances mécaniques des mélanges cimentaires, PhD Thesis (in French), Université de Cergy Pontoise, France, 2001.
[17] H. Uchikawa, S. Hanehara, H. Hirao, Influence of microstructure on the physical properties of concrete prepared by substituting mineral powder for part of fine aggregate, Cem. Concr. Res. 26 (1) (1996) 101–111.
[18] E. Zielinska, The influence of calcium carbonate on the hydration process in some Portland cement constituents ($3CaO,Al_2O_3$ and $4Ca,Al_2FeO_3$), Pr. Inst. Technol. Prod. Bud. (3) (1972).
[19] I. Soroka, N. Stern, Calcareous fillers and compressive strength of Portland cement, Cem. Concr. Res. 6 (1976) 367–376.
[20] R.F. Feldman, V.S. Ramachandran, P.J. Sereda, Influence of $CaCO_3$ on the hydration of $3CaO,Al_2O_3$, J. Am. Ceram. Soc. 48 (1) (1965) 25–30.
[21] H. Moosberg-Bustnes, B. Lagerblad, E. Forssberg, The function of fillers in concrete, Mat. Struct. 37 (2004) 74–81.
[22] A.M. Poppe, G. De Schutter, Cement hydration in the presence of high filler contents, Cem. Concr. Res. 35 (2005) 2290–2299.
[23] P. Lawrence, M. Cyr, E. Ringot, Mineral admixtures in mortars: effect of type, amount and fineness of fine constituents on compressive strength, Cem. Concr. Res. 35 (2005) 1092–1105.
[24] Philippe Lawrence, Sur l'activité des cendres volantes et des additions minérales chimiquemebnt inertes dans les matériaux cimentaires, Université Paul Sabatier/ Toulouse, France, PhD Thesis (in French), 2000.
[25] J. Pera, S. Husson, B. Guilhot, Influence of ground limestone on cement hydration, Cem. Concr. Compos. 21 (1999) 99–105.
[26] V.S. Ramachandran, Thermal analysis of cement components hydrated in the presence of calcium carbonate, Thermochim. Acta 127 (1988) 385–394.
[27] G. Dreux, Contribution à l'étude de l'influence de la finesse des sables sur diverses qualités des bétons, Annales de l'ITPB n.261 (in French), 1969.
[28] S. Tsivilis, E. Chaniotakis, G. Batis, C. Meletiou, V. Kasselouri, G. Kakali, A. Sakellariou, G. Pavlakis, C. Psimadas, The effect of clinker and limestone quality on the gas permeability, water absorption and pore structure of limestone cement concrete, Cem. Concr. Res. 21 (1999) 139–146.
[29] V. Bonavetti, H. Donza, G. Menendez, O. Cabrera, E.F. Irassar, Limestone filler cement in low w/c concrete: a rational use of energy, Cem. Concr. Res. 33 (2003) 865–871.
[30] R. Dupain, R. Lanchon, J.C. Saint-Arroman, Granulats, Sols, Ciments et Bétons: Caractérisation des matériaux de Génie Civil par les essais de laboratoire, Casteilla Ed., Paris, 1995 Available online (in French) at: http://www.la.refer.org/materiaux.
[31] M. Emerson, Mechanisms of water absorption by concrete, in: R. Dhir, J. Green (Eds.), Proceedings of the International Conference on Protection of Concrete, Univ. of Dundee, Chapman and Hall, 1990, pp. 689–700.
[32] F. Agostini, Z. Lafhaj, F. Skoczylas, H. Loodsveldt, Experimental study of accelerated leaching on hollow cylinders of mortar, Cem. Concr. Res. 37 (1) (2007) 71–78.
[33] H. Loosveldt, Z. Lafhaj, F. Skoczylas, Experimental study of gas and liquid permeability of a mortar, Cem. Concr. Res. 32 (2002) 1357–1363.
[34] C.A. Davy, F. Skoczylas, J.D. Barnichon, P. Lebon, Permeability of macro-cracked argillite under confinement: gas and water testing, Phys. Chem. Earth 32 (2007) 667–680.
[35] I.J. Klinkenberg, The permeability of porous media to liquids and gases, API Drilling and Production Practices, 1941, pp. 200–213.
[36] S. Kolias, C. Georgiou, The effect of paste volume and of water content on the strength and water absorption of concrete, Cem. Concr. Comp. 27 (2005) 211–216.
[37] A. Notat, Interactions between chemical evolution (hydration) and physical evolution (setting) in the case of tricalcium silicate, Mat. Struct. 27 (168) (1994) 187–195.
[38] A. Bessa-Badreddine, Etude de la contribution des additions minérales aux propriétés physiques, mécaniques et de durabilité des mortiers, PhD Thesis (in French), Université de Cergy Pontoise, France, 2004.
[39] J. Baron, A. Raharinaivo, Textbook in Civil Engineering for the *Agrégation* (in French), ENS Cachan, France, 1980-1981.
[40] P. Hawkins, P. Tennis, R. Detwiler, The use of limestone in Portland cement: a state-of-the-art review, Portland Cement Association, 2003 Report n. EB227.
[41] P. Poitevin, Limestone aggregate concrete, usefulness and durability, Cem. Concr. Comp., 21 (1999) 89–97.
[42] V. Boel, K. Audenaert, G. De Schutter, G. Heirman, L. Vandewalle, B. Desmet, J. Vantomme, Transport properties of self compacting concrete with limestone filler or fly ash, Mat. Struct. 40 (2007) 507–516.
[43] S.K. Agarwal, D. Gulati, Utilization of industrial wastes and unprocessed micro-fillers for making cost-effective mortars, Cons. Build. Mat. 20 (2006) 999–1004.
[44] G.C. Isaia, A.L.G. Gastaldini, R. Moraes, Physical and pozzolanic action of mineral additions on the mechanical strength of high-performance concrete, Cem. Concr. Comp. 25 (2003) 69–76.